Dynamic Viscosity of Colloidal Silica Suspensions at Low and High volume fractions

Siamak Samavat[a]*, Félix Carrique[b], Emilio Ruiz-Reina[c], Wei Zhang[a], Paul Melvyn Williams[a]

[a] College of Engineering, Swansea University, Bay Campus, Fabian Way, Swansea SA1 8EN, UK

[b] Departamento de Física Aplicada I, Facultad de Ciencias, Universidad de Málaga, Campus de Teatinos, 29071 Málaga, Spain

[c] Departamento de Física Aplicada II, Escuela de Ingenierías, Universidad de Málaga, Campus de Teatinos, 29071 Málaga, Spain

*Corresponding author: s.samavat@swansea.ac.uk

Abstract

A comprehensive study was carried out on the dynamic viscosity of X30 silica dispersions at both high and low volume fractions of colloidal silica particles at various electrolyte ionic strength and pH values. Booth and Ruiz-Reina and Carrique theoretical models (R-R&C) were compared in predicting the primary electroviscous effect (PEE) for viscosity at low volume fractions. To this respect the colloidal dispersion was well characterised with regards to electrolyte properties such as the Debye length, κ^{-1}, calculated from the ionic strength, and zeta potential, ζ, calculated from the electrophoretic mobility using the full numerical model by O'Brien and White (O'B&W). R-R&C hard sphere model (which is a modified version of Simha hard sphere model that includes a boundary condition by Happel on the outer radius of the cell) and the semi-empirical Krieger-Dougherty (K-D) models were fitted to the experimental data at high volume fractions. At both low and high volume fractions the viscosity increased with pH and decreased with ionic strength. At low volume fractions both theoretical models significantly underestimated the experimental dynamic viscosities obtained in this work. This could be attributed to the fuzzy structures for silica particles in aqueous conditions reported previously in the literature, where a significantly larger electroviscous parameter, p, was obtained experimentally for silica particles. The

experimental electroviscous parameter, p_{exp}, in this work was found to be roughly an order of magnitude up to 26 times larger than that predicted by Booth and around 5±1 times larger than the predicted p by R-R&C model allowing the introduction of a correction factor in the PEE coefficient obtained from R-R&C model enabling good prediction for X30 silica dispersions by the latter model. The significant improvement of the electroviscous effect predictions by R-R&C model compared to Booth model may be attributed to the limitations invalidating the Booth model at the electrolyte conditions in this study. At high volume fractions, the R-R&C hard sphere cell model, gave a much better fit to the experimental data compared to the K-D model, which also had the advantage of being only dependent on a coefficient that linearly relates an effective volume fraction postulated for the fuzzy silica particles to the experimental. The K-D model however, depends on the intrinsic viscosity, [η], which requires the calculation of the experimental slope of the dynamic viscosity against volume fraction in the dilute limit, and also on a maximum packing fraction as a fitting parameter. Due to the effect of the fuzzy structures on the viscosity, the latter effective volume fraction ϕ_{eff} was calculated using two approaches: i) as a fitting parameter by fitting the R-R&C hard sphere model to the experimental viscosity data over the entire volume fraction range, and ii) by fitting only the linear part of the experimental viscosity at low volume fractions, It is concluded that the R-R&C hard sphere model with the effective volume fraction accounting for the fuzzy structures fits reasonably well the full range of experimental results at low and high volume fractions. When the model is used with the Adamczyk effective volume fraction (*i.e*, considering only the dilute region in the fitting procedure), the predictions get worse at high volume fractions where huge deviations from the experimental results are found upon the increase of pH.

Keywords:
dynamic viscosity; silica dispersion; primary electroviscous effect (PEE); cell model, core shell model.

1 Introduction

Colloidal nanoparticles have attracted increasing attention as a raw material in nanotechnology applications due to their unique properties such as thermal conductivity [1] as well as their stability in suspension [2, 3]. The broad applications of colloidal systems in

various industrial sectors such as food, pharmaceuticals, cosmetics, ink, rubber, water treatment etc., as well as many natural phenomena such as the special characteristics of sand in sea water has drawn the attention of many scientists to colloidal systems. The nature of colloidal suspensions, mainly as a result of nano particles dispersed in a continuous media introduces new characteristics and behaviours, different from normal solutions containing molecules and ions. This enhanced behaviour of the colloidal systems is most apparent when the colloidal particles are forced to flow through a pipe, a capillary, or nano pores of a filtration membrane.

A chemical engineering process which incorporates the flow of a colloidal suspension, such as transportation and filtration, the viscosity of the suspension is significantly important. Economic optimization of these industrial processes necessitates an understanding of the products physical and electrical specifications. Measurements of the viscosity data for a colloidal suspension at different conditions can be significantly time consuming.

Besides, as demonstrated by previous experimental work [4-8], a small change in any of the electrochemical conditions such as pH or ionic strength of the suspension can make a significant difference in the physical properties of the sample which will affect the viscosity of the suspension dramatically. For example an ultrafiltration model was developed by Bowen and Williams [9] based on the assumption of viscosity being constant for various electrical properties of the dispersion and only low volume fractions was considered both of which points to the lack of experimental data on dynamic viscosity. This model can be applied in membrane filtration processes which are crucial to many industrial sectors such as food, water treatment, pharmaceuticals and many more.

It was reported previously that the particle interactions in a colloidal suspension are influenced by the electrical charge on the surface of the particles suspended in the bulk media [10-13]. These interactions enhance the viscosity of the suspension [14]. Such phenomenon is known as the ‘primary electroviscous effect’ (PEE) for the dilute limit of colloids where the dynamic viscosity versus volume fractions is a linear function [15-19]. At higher volume fractions this function becomes non-linear were the double layers overlap and this second effect is called the ‘secondary electroviscous effect’ (SEE) [13, 20-22].

The process of gaining these data is very time consuming and in most cases a significant amount of preparation is required to achieve the desired solution conditions for the viscosity measurements. This certainly motivated many to attempt modelling the viscosity of colloidal suspensions for various electrical conditions. On the other hand, the theoretical models for the viscosity behaviour are very complicated or only apply at low concentrations [15-17, 22-25] and in some cases even at low concentrations these models do not compare with the experimental dynamic viscosity obtained for the widely used silica dispersions. experimental results [5, 26]. This motivated the current work to focus on silica dispersions.

In the past few decades a small number of experimental studies have been carried out on dynamic viscosity of well characterised spherical latex and silica suspensions at various pH or ionic strength values which focused on low volume fraction PEE theoretical models [4-8, 27]. However, to date no experimental work has evaluated the most recent state of the art theoretical model developed by Ruiz-Reina and Carrique [28] and its improvement from the well-known model by Booth [16]. In some cases the theory has not been compared to the experimental data at all [17, 19, 22].

On the other hand, a few experimental studies were performed to validate the models on the dynamic viscosity of colloidal suspensions at high volume fractions [5, 29-40] the majority of which were only compared to the Krieger-Dougherty model [5, 34-40]. The simplified hard sphere version of Ruiz-Reina and Carrique (R-R&C) [22], as a modified version of the original Simha model [41] however, was not examined by any experimental work to this date. Considering the R-R&C hard sphere cell model (similar to the original Simha model) can be explored to fit the experimental data incorporating one fitting parameter which can be introduced to the R-R&C hard sphere model as a correction factor as opposed to Krieger-Dougherty which includes two fitting parameters, the comparison between the two models for higher volume fractions would be valuable. Finally, only the work of Adamczyk *et al.* was found to study both low and high volume fractions, however, at very few electrolyte conditions [5]. Adamczyk and Laven & Stein reported an experimental PEE coefficient (p) to deviate from Booth predictions due to a fuzzy structure for silica particles once in electrolyte [5, 16, 26]. This motivated the study of silica dispersions in particular to challenge the state of the art models in predicting the unusually large dynamic viscosities observed experimentally.

The present work evaluates a wholesome study on the dynamic viscosity of well characterised colloidal silica dispersions against both low and high volume fractions at two electrolyte ionic strengths and three pH conditions for each electrolyte concentration. The zeta potential is estimated from electrophoretic mobility values using a suitable model after comparisons between a number of well-known models [42-47]. A number of well-known models (as shown in Table 1) related to both linear (low volume fraction which are discussed in details in the Supporting Information File: Section 1) and non-linear (high volume fraction) regions of the viscosity curves were assessed against the experimental data. For the linear part (PEE) at low volume fractions the Booth equation [16, 48] was compared to the numerical solution by Ruiz Reina *et al.* [22] in predicting the experimental data. Regarding the non-linear part at high volume fractions, the empirical expression by Krieger-Dougherty [35] was fitted to the experimental data by varying the maximum packing fraction ϕ_m as a fitting parameter. Also, the R-R&C hard sphere model (a modified version of the Simha hard sphere model which includes a boundary condition by Happel on the outer radius of the cell [22, 41] was fitted to the experimental viscosities by effective volume fractions that take into account the postulated fuzzy structure of silica particles. This study aimed at identifying the most suitable models for the linear viscosity range at low volume fractions as well as the non-linear range at high volume fractions at two ionic strength and three pH electrolyte conditions.

2 Theoretical Aspects

The electrical contribution to the viscosity of colloidal suspensions is mainly dependant on the charge determining ions on the surface of the colloidal particles as well as the ionic strength of the counter-ions present in the electrolyte [10]. Therefore, the effect of ζ-potential on the particles and ionic strength of the electrolyte needs to be observed over a wide range of volume fractions of colloids.

The classic model for predicting the dynamic viscosity behaviour of rigid particles without surface charge was originally proposed by Einstein in 1906 [49] in which the repulsive electrostatic interactions between the particles was not taken into account:

$$\text{Einstein hard sphere model: } \eta_{sp} = \frac{5}{2}\phi \tag{1}$$

where, ϕ is the volume fraction of the dry particles, and η_{sp} is the specific viscosity:

$$\eta_{sp} = \eta_r - 1 = \frac{\eta}{\eta_0} - 1 \tag{2}$$

and, η and η_0 are the dynamic viscosity of the colloid and the electrolyte respectively.

In 1916 a model was proposed by Smoluchowski as shown in Table 1 considering the relative size of the particles to electrical double layer (EDL) and zeta potential at the slipping plane (surface potential) of colloidal particles [15]. This was not only the pioneer model indicating the significance of electrical properties but also led to definition of the so called primary electroviscous effect (PEE) where the viscosity deviates from Einstein model in equation (1) which drew the attention of experimentalists [4, 27]. The PEE by definition, refers to distortion of the double layer due to shearing processes against the electrolyte molecules which leads to an increase in dynamic viscosity [14]. In general the PEE applies to low volume fractions where the colloidal particles' double layers do not overlap due to a much larger distance between the particles and only particle-electrolyte interactions occur [10]. The dynamic viscosity is a linear function at low volume fractions from which the slope is defined as intrinsic viscosity *i.e.*:

$$[\eta] = \frac{d\eta}{d\phi} \tag{3}$$

The Einstein equation for the linear viscosity behaviour for low volume fractions can therefore be written with respect to intrinsic viscosity:

$$[\eta] = \frac{5}{2} \tag{4}$$

And the contribution of the PEE may be defined as:

$$\eta_{sp} = \frac{5}{2}\phi(1+p) \tag{5}$$

where, p is known as the PEE coefficient.

In 1948 Booth modified Smoluchowski's electrical term as shown in Table 1 applying an equations of motion series which was then simplified via a number of assumptions [16, 48, 50]. These terms presented by the Booth equation in Table 1 involved a relaxation function,

$\{Z(\kappa a)\}$ which was a power series of the Debye-Hückel parameter, κa as particle size to double layer thickness ratio (κ is reciprocal of the double layer thickness, and a is the particle size radius), and electrical to kinematic energies ratio, $\frac{e\zeta}{kT}$ (e is charge of an electron, ζ is surface potential, k is the Boltzmann constant, and T is temperature). Since Booth equation was proposed, several attempts were made to predict PEE at low volume fractions, of which the Watterson and White numerical model [17] was found to behave quite similar to the Booth equation and underestimate the PEE even more for some electrolyte conditions [15-19, 27, 51-62] (see Table S1). On the other hand, the Booth model agreed quite well with the experimental viscosity of polystyrene lattices obtained by Stone-Masui in 1968 [4].

In 1952 Simha introduced a cell model [41] suitable for high volume fractions representing units of bulk electrolyte with one particle per unit cell as shown in **Error! Reference source not found.**. A critical ratio, b/a was defined in Simha's model where a and b were the particles hydrodynamic radius and the radius of the cell unit, respectively. This ratio can be expressed as a function of the volume fraction and the maximum packing fraction of the nano particles, ϕ_m, as a fitting parameter. Happel also proposed a cell model [63] which unlike Simha's expression did not simplify to Einstein's equation at boundary condition $\phi \to 0$ which made Simha's approach more suitable for future development.

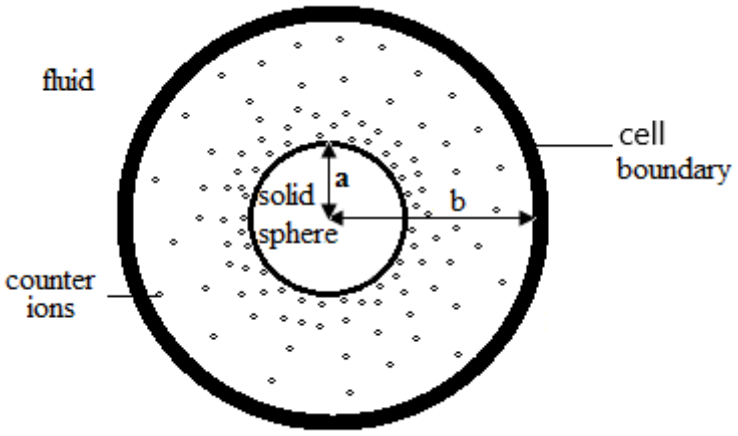

Figure 1: The cell model diagram for a single spherical particle in an electrolyte.

Later on Simha's cell model was used in combination with the electroviscous effect by a number of PEE theoreticians [22-24, 28, 64, 65] among which the most recent work proposed a numerical solution developed by Ruiz-Reina and Carrique in 2007 [28, 64, 66] as shown in

Table 1. This model included overlapping conditions at low salt concentrations where most previous models fail due to the assumption of thin double layers in their derivations.

In 1959 Krieger and Dougherty (K-D) derived a power expression for high volume fractions defining a maximum packing volume fraction, ϕ_m as a fitting parameter [35]. The K-D model introduced an intrinsic viscosity, [η] parameter, *i.e.* the experimental slope obtained from the linear part of dynamic viscosity curve at low volume fractions. The K-D model was in good agreement with previous experimental data [32, 35, 67] which should be the case considering this model is a fit to the experimental data. In 1977 Quemada developed a similar expression for uncharged hard spheres [29]. Also Ball and Richmond introduced a similar expression in 1980 using a crowding factor k_m which was essentially ϕ_m^{-1} [67]. The intrinsic viscosity in Quemada and Ball and Richmond models is a constant, which neglects the PEE in the dynamic viscosity and imposes a limitation in curve fitting of those models.

Adamczyk and Laven & Stein studies reported the unusually large dynamic viscosities for silica dispersions attributed to the gel-like fuzzy structure of silica in aqueous conditions as shown in Figure 2even at low volumes fractions [5].

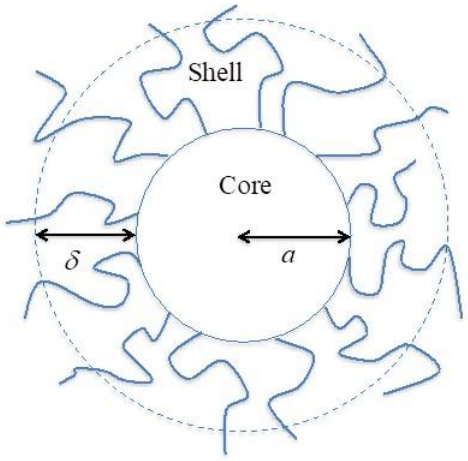

Figure 2: A possible formation of a silica particle in an aqueous electrolyte proposed similarly by Adamczyk *et al*. [5].

The proposed model by Adamczyk is discussed in details in the following sections and shown in brief in Table 1.

Table 1: A summary of the theoretical and empirical models evaluated in this study for low and high volume fractions:

Low Volume Fraction Models

Einstein (1906):

$$[\eta] = \frac{5}{2}$$

Where, $[\eta] = \frac{d(\eta_{sp})}{d\phi}$, and $\eta_{sp} = \eta_r - 1 = \frac{\eta}{\eta_0} - 1$

Booth (1950):

$$[\eta] = \frac{5}{2}[1 + p_{Booth}]$$

Where $p_{Booth} = \frac{(\zeta\varepsilon)^2}{4\pi\lambda_0\eta_0 a^2}(\kappa a)^2(1+\kappa a)^2\{Z(\kappa a)\}$

Low & High Volume Fraction Models

Krieger-Dougherty (1959):

$$\eta_{sp} = \left(1 - \frac{\phi}{\phi_m}\right)^{-[\eta]_{exp}\phi_m} - 1$$

Ruiz-Reina *et al*. (2005):

$$\eta_{sp} = \frac{5}{2}\phi S(\phi)(1 + p_{R\text{-}R\&C})$$

$$S(\phi) = \frac{4\left(1 - (\phi)^{\frac{7}{3}}\right)}{4\left(1 + (\phi)^{\frac{10}{3}}\right) - 25\phi\left(1 + (\phi)^{\frac{4}{3}}\right) + 42(\phi)^{\frac{5}{3}}}$$

Adamczyk *et al*. effective volume fraction correction (2004):

$$\eta_{sp\,(exp)} = [\eta]_{exp}\phi = \frac{5}{2}\phi_{eff} = \frac{5}{2}k_A\phi$$

Where, k_A can be defined as:

$$k_A = \frac{\phi_{eff}}{\phi} = \frac{[\eta]_{exp}}{2.5} = \left(1 + \frac{\delta}{a}\right)^3$$

3 Materials and Methods

3.1 Silica dispersion preparation

Morisol X30 colloidal silica dispersions were purchased from Morrisons Limited. AR Sodium chloride, HCl, and NaOH were purchased from Fisher Scientific. Deionized water (with maximum conductivity of 2 μS/cm) was produced by reverse osmosis, and ion exchange via a Millipore Elix 3.

Morisol silica dispersions were diluted to the desired volume fractions without any purification since the ionic contaminations after dilution (in the final low volume fraction dispersions) become negligible compared to the ionic strength even in the case of 3 mM NaCl. The pH and conductivity of the dispersions were adjusted to the desired values by measuring and directly adding HCl/NaOH and NaCl respectively to the colloidal suspension under gentle stirring after each addition.

High volume fractions of silica dispersions with various pH and ionic strength were prepared in three stages of purification, pH and ionic strength adjustment, and concentration. In all three steps a cross flow hollow fiber filter (Romicon HF1-43-PM10, KOCH Membrane Systems Co.) was used which was fitted in a benchtop Quixstand ultra-filtration rig. The membrane had a molecular weight cut off of 10 kDa. The filter allows the electrolyte ions to move through the filter as permeate and the silica particles will be recirculated in the system as retentate. A Watson Marlow 313S peristaltic pump was used to pump the dispersion in a silicone tube. To enhance the filtration rate, a positive pressure of 2 bars is applied across the filter between pressure gauges 1 and 2 as shown in Figure 3.

For each pH and ionic strength condition 400 g of Morisol silica dispersions were first purified with about 2 litres of deionized (DI) water using a cross flow system shown in Figure 3. The conductivity of permeate was constantly monitored until it was as low as 100 μS/cm indicating the ionic impurities are negligible (discussed in details in Supporting Information File: Section 2).

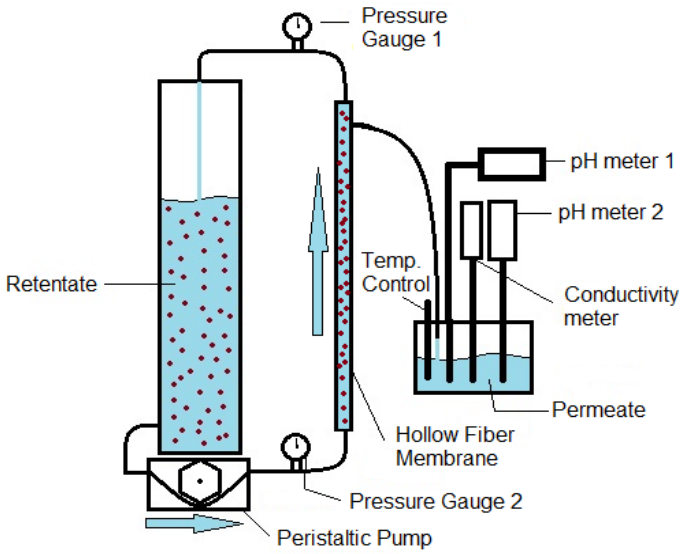

Figure 3: Schematic diagram of the filtration system with controlled temperature and electrical conditions.

The pH and ionic strength of the permeate was continuously monitored using two pH meters (a PW 9421 Philips pH meter and an IQ150 pH meter from IQ Scientific) to ensure the pH readings are accurate. A Portec PI.8140 conductivity meter was used to monitor the ionic strength. Fisher Scientific probes were used for the pH meters (Type No: FB68788) and the Portec conductivity meter (Type No: CDC139/K). The ionic strength adjustment of the retentate was carried out by addition of a calculated magnitude of NaCl according to the conductivity readings of permeate via a method explained in the Supporting Information File: Section 3.

Knowing the approximate weight fraction of the initial colloidal solution and the total weight of the sample, an approximate volume of the desired concentration can be calculated. The electrical properties of the accumulated permeate were recorded at the end of the concentration process. The exact sample concentration in weight % was then calculated by measuring wet and oven dried masses of each end product.

The purified and concentrated dispersion was diluted by adding a known amount of NaCl electrolyte (with a similar NaCl concentration and pH to that of the permeate) to a known mass of the colloidal dispersion. However, the pH may vary during this dilution and a slight readjustment may be required. This normally does not cause any significant variation in the conductivity of the dispersion.

3.2 Weight and Volume Fraction Measurements

The weight fractions of Morisol stock solutions were initially measured. Three samples of Morisol silica solution were weighed in three foil containers. The samples were then placed in an oven and left to dry at 120°C for twelve hours and weighed. The weight fraction of silica was then calculated and averaged. The same method was applied to find the concentration of the purified solutions after filtration. From these weight fractions, the hydrodynamic volume fractions were calculated as described in Supporting Information File: Section 3.

3.3 Density Measurements

A 25ml pycnometer flask was used for the density measurements via the method described in British Standards (BS 4522, 1988). The only variable parameter in the calculation of the density of a colloidal dispersion is the weight of the sample which is used in the equations below:

$$\rho_s = \frac{m_1 + A}{m_2 + A} \times \rho_w \tag{6}$$

$$A = \rho_a \times m_2 \tag{7}$$

where ρ_s is the density of the solution at 25 ± 0.1°C, m_1 is the apparent mass of the sample in grams, m_2 is the apparent mass of the pure water, ρ_w is the density of water at 25°C (0.997044 g/ml) and A is the buoyancy correction, where ρ_a is the density of air at 25°C (1.184 mg/ml). Density data are presented in more details in Supporting Information File: Section 4.

3.4 Viscosity Measurements

In this study dynamic viscosity measurements were carried out for both low and high volume fractions using a range of Ostwald capillary viscometers which provide good sensitivity to small changes in viscosity importantly for low volume fractions as demonstrated in previous literature [4, 6, 8, 27, 68-70]. The *Pe* numbers in all measurements were less than 2.6×10^{-3} demonstrating that the diffusive forces dominate the flow (Supporting Information File: Section 5).

A full description of the method for measuring the viscosity of the dispersions was mentioned in British Standards [71]. The kinematic viscosity was calculated as a function of time using a glass capillary viscometer held vertically in a temperature controlled water bath (25 ± 0.1 °C, Figure 4). The dynamic viscosity was then calculated using the kinematic viscosity and density of the solutions (Supporting Information File: Section 6). The viscosity measurements were carried out on silica X30 dispersions at three pH conditions (pH 9, 7, 5) and two ionic strength conditions (30 mM and 3 mM of NaCl as the electrolyte) i.e. six combinations of electrolyte pH and ionic strength in total.

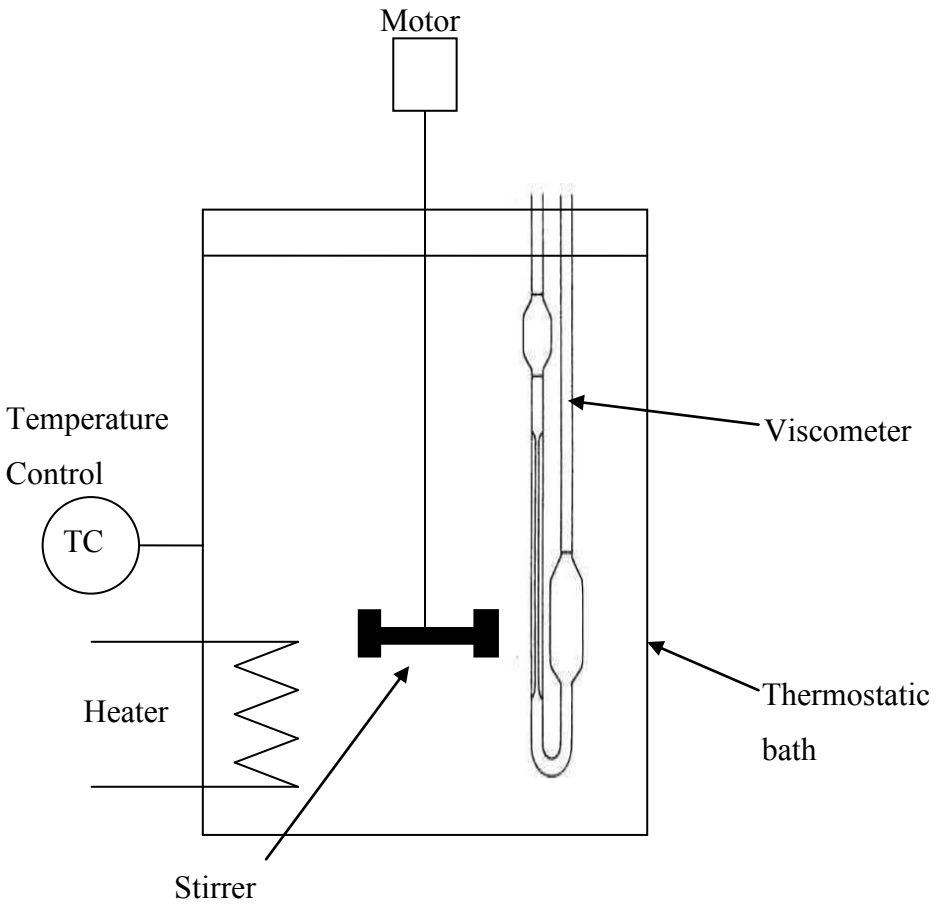

Figure 4: Schematic diagram of the viscosity measurement setup.

3.5 **Colloidal Particle Characterisation**

A Malvern High Performance Particle Sizer (HPPS) incorporating NIBS (Non-Invasive Back Scatter) technology and a Zetasizer Nano ZS were used to measure the hydrodynamic particle size as well as mono-dispersity of Morisol silica dispersions. Prior to the HPPS

measurements, Morisol X30 silica dispersions (4 to 10 g/L) were prepared at each pH and ionic strength condition and were passed through an Acrodisc 25 mm syringe filter (with 1 μm glass fiber membrane, from PALL life sciences) to remove any undesirable particles.

A scanning electron microscope (col/FEG SEM S4800) was used to observe the dry particle size, mono dispersity, and morphology of X30 silica nanoparticles. Prior to SEM imaging, samples were prepared by drop-casting 0.5 mL of X30 silica dispersion (0.1 g/L) onto silicon wafer followed by oven drying at 150 °C overnight.

The electrophoretic mobility, u_E, of X30 silica dispersions were measured using a Malvern ZetaMaster 2000. For each condition a known volume of the dispersion was injected into the cell capillary and the mobility values were averaged over a minimum of thirty measurement runs. The zeta potential of the silica dispersions was then obtained from the electrophoretic mobility values using O'B&W numerical model after comparing with some other well-known models [42-47].

4 Results and Discussions

4.1 Particle characterisation

The hydrodynamic and dry particle size for silica X30 particles is shown in Table 2. Figure 5 confirms the mono-dispersity of these particles. The dry particle size was the average of measurements taken from the SEM images shown in Figure 4. It can be seen that the SEM average dry particle size from the SEM imaging is quite similar to the average hydrodynamic particle size from DLS measurements. However, the DLS measurements were carried out in the same aqueous conditions as the viscosity measurements, and the hydrodynamic radius obtained from this method showed a much smaller standard deviation compared to the SEM observations. Therefore, the hydrodynamic radius obtained from the DLS measurements was used in all viscosity models.

Table 2: Particle size characterization.

	Hydrodynamic particle size (DLS)		Dry size (SEM imaging)
Particle type	Particle radius (nm)	Average poly-dispersity index	Particle radius (nm)
X30 Silica	10.68 ± 0.28	0.19 ± 0.03	11.8 ± 2.4 (averaged using measurements in Figure 5)

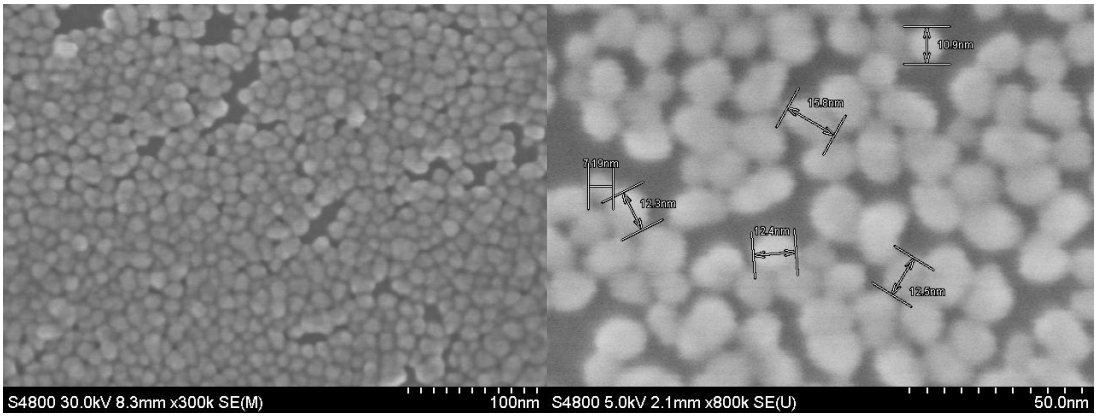

Figure 5: (left panel) X30 particles (300k magnification); (right panel) with approximate particle size measurements (800k magnification).

4.2 **Effects of pH and ionic strength on specific viscosity**

The experimental data are compared at constant ionic strength and variable pH values. The experimental dynamic viscosity, η_{exp}, was normalised to experimental specific viscosity, $\eta_{\text{sp (exp)}}$, as previously defined in the literature [6]:

$$\eta_{\text{sp (exp)}} = \eta_{\text{exp}} / \eta_{\text{NaCl}} - 1 = \eta_{\text{r (exp)}} - 1 \tag{8}$$

where η_{exp} is the experimental dynamic viscosity and η_{NaCl} is the respective solvent viscosity. As shown in Figure 6 the specific viscosity increased when increasing pH. For instance, at 30 mM NaCl and ϕ = 0.3 the viscosity was more than doubled when pH was increased by two units and more than tripled when increasing pH a further two units. This effect was almost similar at lower ionic strength (3 mM NaCl) and ϕ = 0.27 where from pH 5 to 7 viscosity was more than doubled and from pH 7 to 9 it was more than tripled. Also, for

each pH condition the dynamic viscosity was increased with decrease in ionic strength.

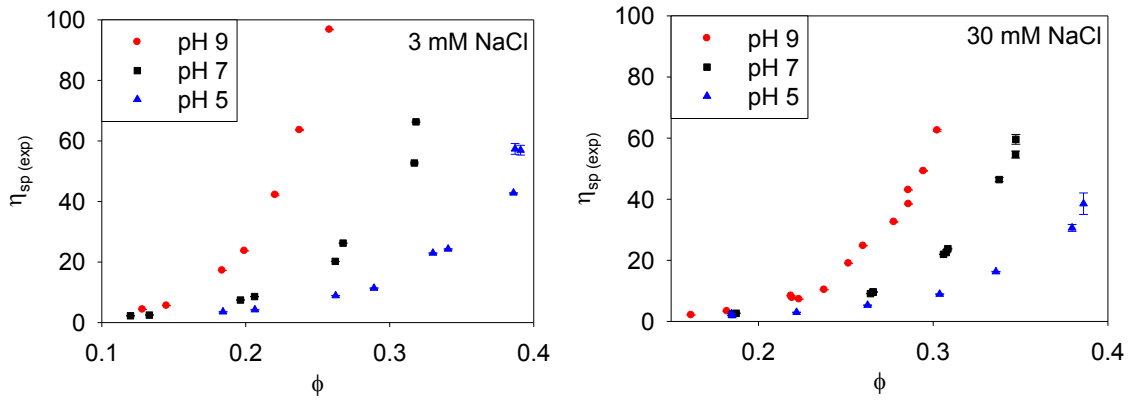

Figure 6: Comparison between the experimental data (n=3) of specific viscosity for X30 silica at different pH values and ionic strengths. Left panel: c = 3 mM, right panel: c = 30 mM.

4.3 Low volume fraction Intrinsic Viscosity (PEE)

The viscosity of a colloidal solution at low volume fractions was originally calculated by Einstein's (1906, 1911) linear equation [49, 72] where the intrinsic viscosity predicted by Einstein was 2.5. For our low volume fraction viscosity data we explore a similar equation:

$$\eta_{\exp} = \eta_{\mathrm{NaCl}}\left(1+\phi[\eta]\right) \tag{9}$$

This equation can be rearranged and combined with equation (3) to give:

$$[\eta]_{\exp} = \frac{d\left(\eta_{\mathrm{sp\,(exp)}}\right)}{d\phi} = \text{ The linear slope of } \eta_{\mathrm{sp\,(exp)}} \text{ vs. } \phi \tag{10}$$

The experimental intrinsic viscosity values, $[\eta]_{\exp}$ calculated from experimental data were different from Einstein's prediction, and were then compared to Booth and R-R&C theoretical models [15, 16, 66] as shown in Figure 7. The colloidal dispersion properties such as pH, zeta potential, κa, as well as experimental intrinsic viscosity, and ratios of experimental PEE coefficients to the predicted ones by Booth and R-R&C were shown in Table 3. The zeta potential values were obtained from ζ obtained from the electrophoretic mobilities using the full numerical model by O'Brien and White after comparison with other well-known models (for details see Supporting Information File: Section 7). The $[\eta]_{\exp}$ experimental values were used in Krieger-Dougherty model for high volume fractions as one of the fitting parameters.

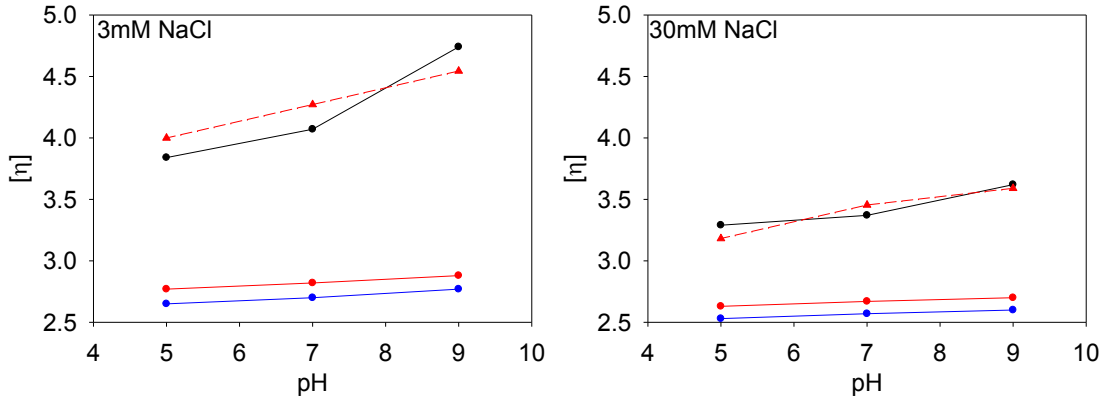

Figure 7: Experimental intrinsic viscosity at various pH for low volume fractions (black, solid line) compared to Booth model (blue, solid line), R-R&C model (red, solid line), and R-R&C model with 5.45 correction according to equation (11) (red, dashed line). Left panel: c = 3 mM, right panel: c = 30 mM.

Table 3: Experimental intrinsic viscosities at various pH and ionic strengths as well as the ratio of experimental PEE coefficients to theoretical ones. Some more details are given in the Supporting Information File: Section 8.

Case No:	NaCl Electrolyte Ionic Strength (mmole·L^{-1})	pH (-)	κa (-)	$\zeta_{O'B\&W}$ (mV)	$[\eta]_{exp}$ (-)	p_{exp} / p_{Booth} (-)	p_{exp} / $p_{R\text{-}R\&C}$ (-)
1	3	9	1.92	-66.35	4.74	8.2	6
2	3	7	1.92	-57.6	4.07	7.9	4.8
3	3	5	1.92	-50.31	3.84	9	4.9
4	30	9	6.08	-54.66	3.62	11.3	5.6
5	30	7	6.08	-44.8	3.37	12.5	5
6	30	5	6.08	-28	3.29	26.66	6.4

As shown in Figure 7 both models significantly underestimate the experimental intrinsic viscosities for all conditions. This large deviation from the theoretical data was found in

previous literature mainly by the work of Adamczyk *et al*. [5] as well as Laven and Stein [26] for silica colloidal dispersions. The discrepancies between the R-R&C and the experiments are discussed in more depth in the next section.

In comparison between the two theoretical models, the numerical model by R-R&C [22, 28] generally showed slight improvement of the intrinsic viscosity for all conditions yet well below the experimental values for all conditions. In addition, the ratio of experimental PEE values, p_{exp}, to that of Booth and R-R&C models were shown in Table 3. It was observed that Booth model underestimated the PEE by an order of magnitude for most cases whereas R-R&C model underestimated the PEE by roughly 5.5 times. Interestingly, one can observe from Table 3 that the $p_{\text{exp}} / p_{\text{R-R\&C}}$ ratio is almost constant for all cases unlike large variations in $p_{\text{exp}} / p_{\text{Booth}}$. One may obtain an average $p_{\text{exp}} / p_{\text{R-R\&C}}$ which could be used as a correction factor for $p_{\text{R-R\&C}}$ in the R-R&C equation for predicting the viscosity of silica X30 dispersions at low volume fractions:

$$\eta_{\text{sp}} = \frac{5}{2}\phi S(\phi)\left(1 + p^{*}_{\text{R-R\&C}}\right) \tag{11}$$

where $p^{*}_{\text{R-R\&C}} = 5.45 \times p_{\text{R-R\&C}}$. On the other hand, the large $p_{\text{exp}} / p_{\text{Booth}}$ values may be reflect the limitations in Booth model failing to predict the PEE. In developing the equations of motion, Booth applied a few assumptions for the particle-electrolyte interface [16] of which perhaps the assumption of the double layer being small in thickness compared to the average distance between the particles had the most impact to underestimate the double layer effects even for low volume fractions. Also the modified Booth model used in this study as shown in Table 1 is restricted to zeta potential values less than 25.4 mV which is less than all the observed values in this work as shown in Table 3. Since the numerical solution by R-R&C model are not limited by these assumptions it is expected to see improvement in the viscosity predictions.

In summary, despite the improvement of the PEE parameter, *p*, by R-R&C model as shown in Table 3, both theoretical models fail to predict the intrinsic viscosities by a significant margin as shown in Figure 7 which was reported in the literature to be due to the fuzzy structure of silica particles in aqueous media [5, 26]. The numerical solution by Ruiz-Reina and Carrique [22, 28] marginally improved the predicted intrinsic viscosities and the PEE parameter, *p*, significantly from Booth equation. Also a correction factor of 5.45 was necessary for the R-

R&C model to match the experimental viscosities of silica X30 samples at low volume fractions, in spite of the R-R&C model is intended to be valid for non-dilute suspensions and arbitrary zeta potentials, even for the cases of overlapping of neighbour EDL's.

4.4 **High Volume Fraction Viscosity**

In the present section we will study and compare some theoretical and semi-empirical approaches to the experimental specific viscosity of the X30 Silica suspensions in the region of high-volume fractions.

First of all, we have tested in Figure 8 whether the electroviscous R-R&C model [22, 28] is able to predict the experimental results for different pH and ionic strength conditions. This model predicts the viscosity of a concentrated colloidal suspension of charged spherical particles including electroviscous effects linked to electric body forces in the double layers, and possible overlapping between adjacent double layers of neighbor particles. As it is clearly observed in Figure 8, the R-R&C model predicts values well below the experimental ones. Also, in this Figure, R-R&C hard sphere results (no electroviscous effects included) are displayed for the same cases to show that the complete R-R&C prediction hardly differs from the simpler hard sphere one. These results show similar behavior to the low volume fraction viscosities in which the R-R&C model values are well below the experimental values even for the pH5, 30mM ionic strength case. For clarity, the two predictions are reproduced here:

$$\text{R-R\&C model: } \eta_{sp} = \frac{5}{2}\phi S(\phi)\left(1 + p_{\text{R-R\&C}}\right) \tag{12}$$

$$\text{R-R\&C hard sphere model: } \eta_{sp} = \frac{5}{2}\phi S(\phi) \tag{13}$$

being $p_{\text{R-R\&C}}$ the electroviscous coefficient which in this case encompasses all the electroviscous effects. In the R-R&C model, the function $S(\phi)$ in Table 1 follows from a modified version of the general Simha function $\lambda(y)$ when a boundary condition by Happel [41] on the outer radius of the cell, $y = a/b = \phi^{1/3}$, is imposed. This boundary condition fixes the radius of the cell by obliging that the particle volume fraction calculated with a single unit cell coincides with the particle volume fraction of the whole suspension.

To explain the discrepancies found between experiments and the R-R&C model we have explored a composite core/shell silica particle model. In the literature [5, 26], some discrepancies with colloidal silica particles between experiment and theory led to the postulation of a fuzzy, gel-like structure, responsible for the large specific viscosity deviations observed. In aqueous solutions, a gel-like layer seems to be formed onto the silica particles. This fact could explain the apparent particle density decrease for low ionic strength and high pH, and also that the thickness of the gel-like layer could apparently be correlated with the double-layer thickness.

Originally, Adamczyk *et al*. [5] confirmed that their experimental results of the specific viscosity didn't follow the Einstein hard sphere model in the low volume fraction region [49, 72]. Next, they tried to explain their experiments in such region making use of primary electroviscous effects implicit in the electroviscous coefficient, *p*, [5] and they found that such electroviscous effects could not be responsible for the observed discrepancies after a theoretical estimation of *p*, that turned out to be two orders of magnitude smaller than those necessary to explain the experiments.

Adamczyk *et al*. [5, 26] finally assumed the above-mentioned fuzzy structure for their silica particles and derived an apparent or effective particle volume fraction: $\phi_{\text{eff}} = k_{\text{A}}\phi$, which depended linearly on the volume fraction, to explain their viscosity experiments in the low volume fraction region. The linear coefficient k_A is obtained from the slope of the linear fit of the experimental specific viscosity, $[\eta]_{\text{exp}}$ versus volume fraction in the latter region:

$$\text{Adamczyk et al. correction: } \eta_{\text{sp (exp)}} = [\eta]_{\text{exp}}\,\phi = \frac{5}{2}\phi_{\text{eff}} = \frac{5}{2}k_{\text{A}}\phi \tag{14}$$

where, k_{A} can be defined as:

$$k_{\text{A}} = \frac{\phi_{\text{eff}}}{\phi} = \frac{[\eta]}{2.5} = \left(1+\frac{\delta}{a}\right)^3 \tag{15}$$

where, a is the dry particle radius, and δ is the thickness of the gel layer around the particle in aqueous conditions. In all their experiments $k_{\text{A}} > 1$, whereas the value expected for k_{A} if the experiments had followed the Einstein viscosity model for hard spheres would be one.

Also, these effective volume fractions were used for the interpretation of their experimental viscosity results in the high-volume fraction region [5]. In their case, the hard sphere model

of Batchelor for low-medium volume fractions range [73] was used in conjunction with effective volume fractions, but it was not sufficient to match their results. The posterior inclusion of a correction accounting for secondary electroviscous effects with Russel theory [20], led to a better comparison for volume fractions lower than 0.2.

With regards to the X30 Silica particles, and following Adamczyk *et al.* insights [5], an effective volume fraction for the high volume fraction region was derived here: $\phi_{\text{eff}} = k\phi$, being the linear k coefficient (examples of the linear fit are provided in Supporting Information File, Section 9, Figure S13) an adjustable parameter that can be obtained by fitting the high-volume fraction specific viscosity experiments with the R-R&C hard sphere model (the electroviscous effects are rather negligible according to Figure 8) for each pH and ionic strength. The linear relation, in the full range, between the estimated effective volume fraction and the experimental volume fraction ϕ, was in agreement with a constant thickness of the gel-like layer δ, being independent of ϕ.

In Figure 8, the fits of the experimental results with the R-R&C hard sphere model with this effective volume fraction correction are shown for all the pHs and ionic strengths studied. They are named:

R-R&C hard sphere with effective volume fraction $\phi_{\text{eff}} = k\phi$

$$\eta_{\text{sp}} = \frac{5}{2}\phi_{\text{eff}}\,\text{S}\left(\phi_{\text{eff}}\right) = \frac{5}{2}\text{k}\,\phi\ \text{S}(k\phi) \tag{16}$$

On the other hand, as Adamczyk *et al*. did in his work with silica particles [5], where the use of effective volume fractions was extended to the high-volume fraction region, in Figure 8 R-R&C hard sphere predictions with Adamczyk *et al*'s effective volume fractions have been included for comparison. They are named:

R-R&C hard sphere with effective volume fraction $\phi_{\text{eff}} = k_{\text{A}}\phi$

$$\eta_{\text{sp}} = \frac{5}{2}\phi_{\text{eff}}\,\text{S}\left(\phi_{\text{eff}}\right) = \frac{5}{2}k_{\text{A}}\phi\ \text{S}(k_{\text{A}}\phi) \tag{17}$$

The k_A coefficients for the X30 Silica studies were obtained from the slopes of the linear fits of the specific viscosity, $[\eta]_{\text{exp}}$ versus volume fraction in the low volume fraction region for all the pHs and ionic strengths studied in this work (see the Supporting Information File, Section 8, Figures S7 to S12 and Table S5).

Finally, the semi-empirical Krieger-Dougherty model (K-D) [37]:

$$\eta_{sp} = \left(1 - \frac{\phi}{\phi_m}\right)^{-[\eta]_{exp}\phi_m} - 1 \tag{18}$$

where, $[\eta]_{exp}$ stand for the experimental slopes defined above and ϕ_m is a maximum packing fraction coefficient to be used as adjustable parameter. In Figure 8 the K-D fits are also shown for all the experimental conditions of pH and ionic strength in the high-volume fraction region. Estimated values for the linear k_A and k coefficients of the effective volume fractions and maximum packing fraction coefficients ϕ_m of the K-D model for the best fits to the X30 Silica experiments are summarized inTable 4.

Table 4: Linear coefficients of the effective volume fraction according the R-R&C hard sphere model, and maximum packing fraction coefficient of the K-D model for best fits to X30 Silica experiments.

Case No:	NaCl Electrolyte Ionic Strength (mmole·L^{-1})	pH (-)	k_A (-)	k (-)	ϕ_m (-)
1	3	9	1.90	2.48	0.26
2	3	7	1.63	1.86	0.33
3	3	5	1.54	1.49	0.43
4	30	9	1.45	1.94	0.31
5	30	7	1.35	1.67	0.36
6	30	5	1.32	1.40	0.41

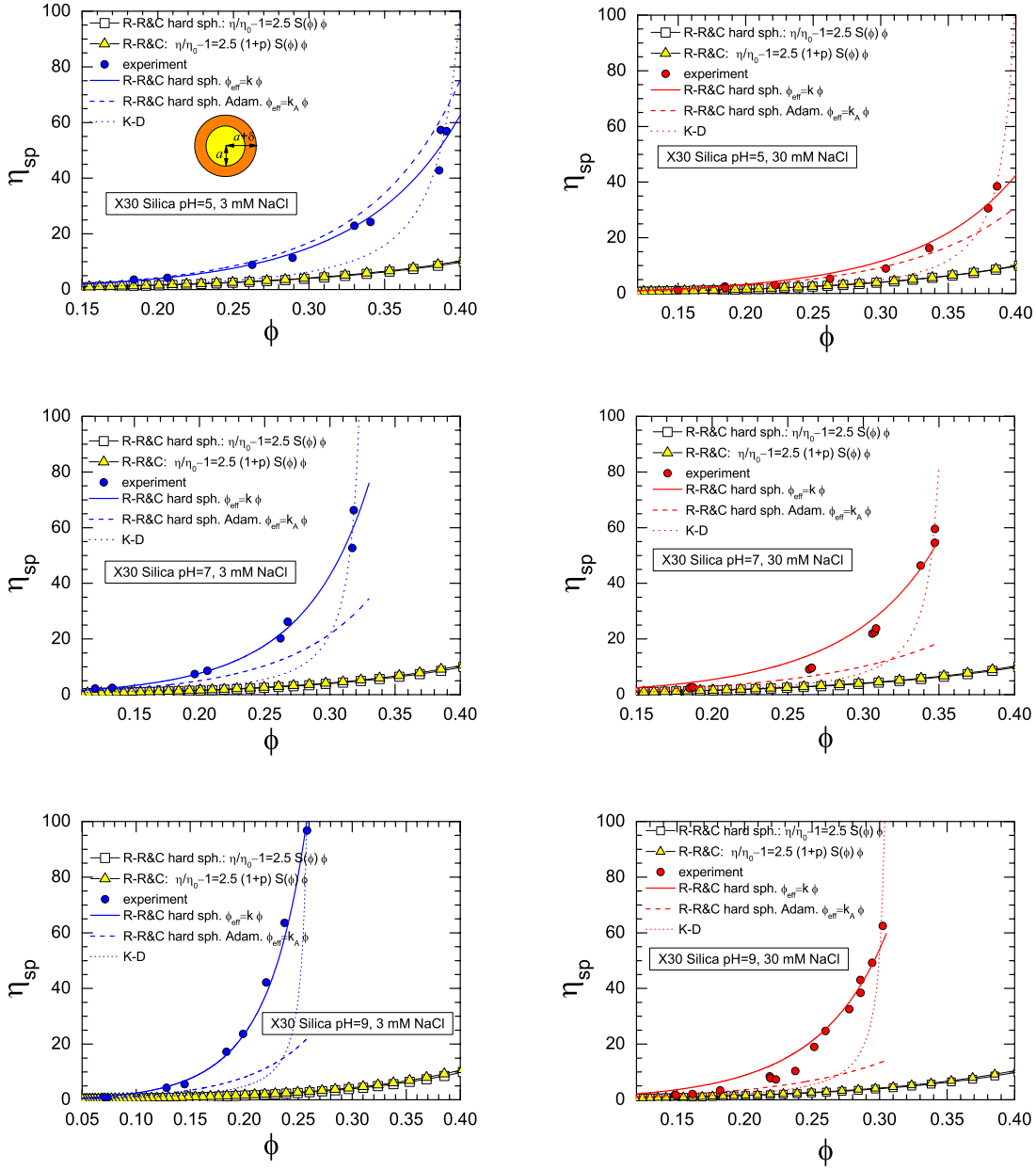

Figure 8: Specific viscosity against volume fractions for X30 silica at all pHs 5,7 and 9 for 3mM and 30mM NaCl concentrations; R-R&C hard sphere model (squares); R-R&C model (triangles); experimental results (circles); R-R&C hard sphere model with effective volume fraction $\phi_{\text{eff}} = k\phi$ (solid lines); R-R&C hard sphere model with Adamczyk *et al*. effective volume fraction $\phi_{\text{eff}} = k_{\text{A}}\phi$ (dashed lines); Krieger-Dougherty (K-D) model (dotted lines). Left panels: c = 3mM, right panels: c = 30mM and Upper panels: pH = 5, middle panels: pH = 7, and lower panels: pH = 9

Whatever the case studied, the best fits to the experimental specific viscosities, especially for 3 mM NaCl ionic strength, are given by the R-R&C hard sphere model with effective volume

fraction $\phi_{\text{eff}} = k\phi$. Adamczyk *et al*'s effective volume fraction does not seem to be a good approach for the high volume fraction studies for pHs larger than 5. Also the K-D fits in Figure 8 are not good enough for adjusting our experiments.

An effective volume fraction can be related to a gel-like layer onto the bare silica particle, its thickness δ according the two approaches can be easily derived:

$$\phi = \frac{N_{\text{p}} \frac{4}{3}\pi a^3}{V_{\text{s}}}; \phi_{\text{eff}} = \frac{N_{\text{p}} \frac{4}{3}\pi (a+\delta)^3}{V_{\text{s}}} \tag{19}$$

where N_{p} is the number of particles and V_S is the suspension volume. As $\phi_{\text{eff}} = C\phi$, ($C$ can be k or k_A in our analysis) then,

$$\frac{\phi_{\text{eff}}}{\phi} = \frac{(a+\delta)^3}{a^3} = \left(1+\frac{\delta}{a}\right)^3 = C \tag{20}$$

then,

$$\frac{\delta}{a} = C^{\frac{1}{3}} - 1 \tag{21}$$

Also, a thickness of the gel-like layer can be obtained for the K-D model [37]:

$$\frac{\delta}{a} = \left(\frac{\phi_{\text{mx}}}{\phi_{\text{m}}}\right)^{\frac{1}{3}} - 1 \tag{22}$$

being ϕ_{mx} the maximum packing fraction attainable for the system. For hard spheres the maximum packing fraction for both face-centered cubic and hexagonal close pack in crystal lattices is 0.7404.

In Figure 9 and Figure 10 (see also Figure S14 of the Supporting Information File, Section 9) the ratios of the thickness of the gel-like layer to the particle radius are displayed as a function of experimental conditions such as zeta potential, pH and ionic strength according to the three approaches described above, to find possible correlations with such properties. Initially, the thickness ratios as a function of zeta potential at fixed ionic strength were studied as shown in Figure 9. For both ionic strengths, 3 and 30 mM NaCl, the thickness ratio increases with zeta potential for all approaches. It is remarkable that the K-D model generally shows the largest thickness ratios, which imply an overestimation in comparison with the R-

R&C approach shown in Figure 8 which fits well with the experimental data. The Adamczyk *et al.*'s approach on the other hand shows the smallest ones, which indicates and underestimation compared to the R-R&C model and it was clearly shown in Figure 8. For fixed ionic strength, it is quite reasonable that the larger the surface potential the thicker the charged gel-like layer surrounding the bare particle.

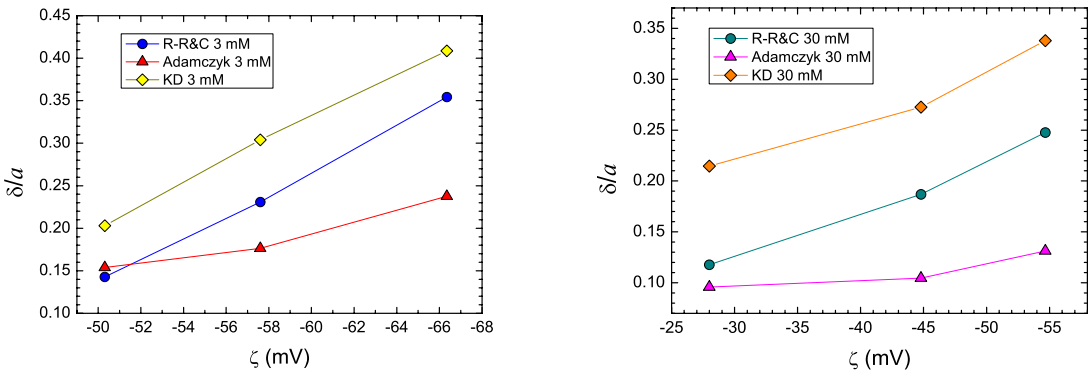

Figure 9: Thickness ratio calculated from R-R&C model with effective volume fraction $\phi_{\text{eff}} = k\phi$, Adamczyk *et al.*'s effective volume fraction $\phi_{\text{eff}} = k_{\text{A}}\phi$, and Krieger-Dougherty (K-D), as a function of zeta potential. Left panel: c = 3 mM NaCl; right panel: c = 30 mM NaCl.

In Figure S14 of the Supporting Information File, Section 9 the thickness ratio is shown as a function of pH at fixed ionic strength. Similar conclusions as the previous Figure can be drawn as zeta potential increases with pH at fixed ionic strength (see Table 4). Finally, in Figure 10 the thickness ratio as a function of ionic strength is displayed for fixed pH. With the exception of the pH5 case in Figure 10, where the K-D ratio increases with ionic strength, unlike the two other approaches, it can be said that overall the thickness ratio decreases with ionic strength at fixed pH. It is probably an effect of the well-known double layer compression with the increase of ionic strength that partially compresses the charged gel-like layer.

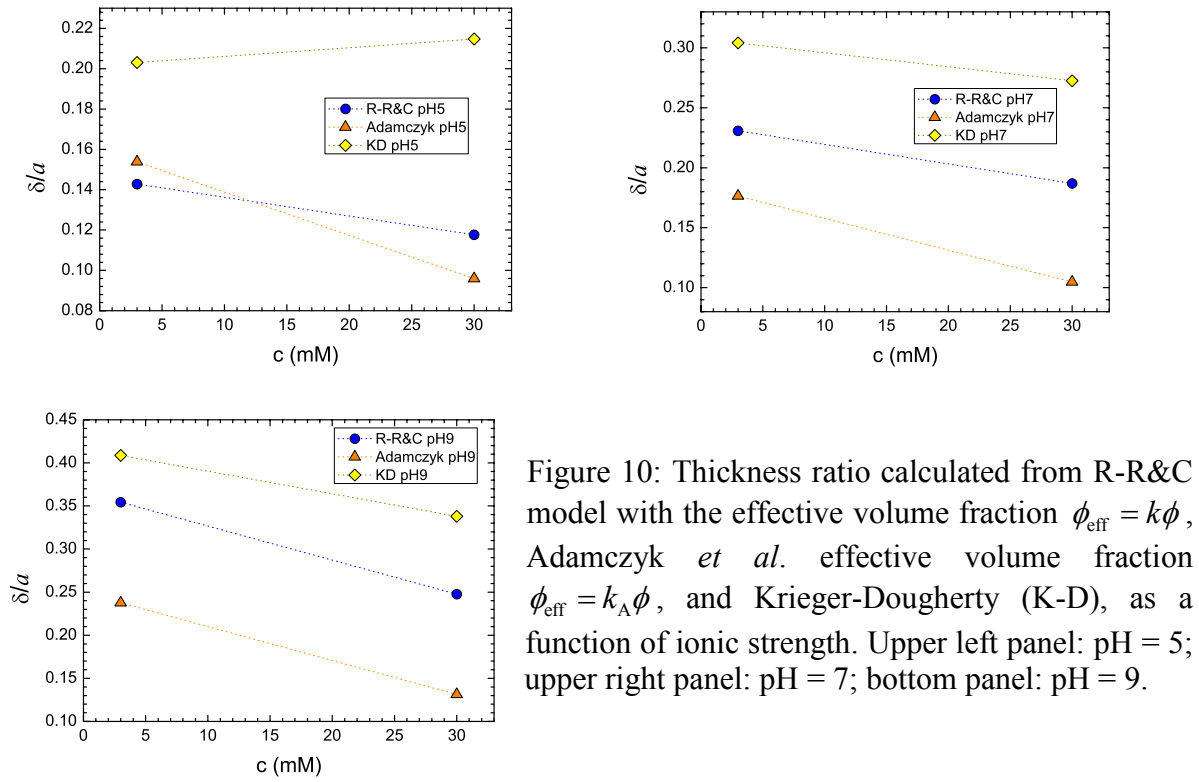

Figure 10: Thickness ratio calculated from R-R&C model with the effective volume fraction $\phi_{\text{eff}} = k\phi$, Adamczyk *et al*. effective volume fraction $\phi_{\text{eff}} = k_{\text{A}}\phi$, and Krieger-Dougherty (K-D), as a function of ionic strength. Upper left panel: pH = 5; upper right panel: pH = 7; bottom panel: pH = 9.

Similar tendencies have been found with aqueous silica sols in the literature. For instance, Adamczyk *et al*. [5] derived K-D thickness ratios of 0.28 and 0.13 for their silica particles at fixed pH = 10 and zeta potentials of –42 mV (ionic strength of 0.02 M) and –35 mV (ionic strength of 0.05 M), respectively. This coincides well with findings in this study in which some correlation between the thickness of the gel-like layer and the double layer-thickness is observed.

5 Conclusion

A comprehensive study was carried out on the dynamic viscosity of X30 silica dispersions at both high and low volume fractions of colloidal silica particles at various electrolyte pH and ionic strength values. The initial results showed a comprehensive trend where lower salt concentration and higher pH led to larger dynamic viscosity of the suspension for both low and high volume fractions.

The experimental findings at low volume fractions were compared with the predictions by Booth and R-R&C theoretical models for which colloidal silica dispersions were well

characterised with respect to the particle size measured using both SEM imaging as well as DLS, Debye length, κ^{-1} was calculated from the ionic strength and zeta potential, ζ obtained from the electrophoretic mobilities using the full numerical model by O'Brien and White after comparison with other well-known models. The first observation from these comparisons was the anomalously larger experimental intrinsic viscosities (slope of the specific viscosities) at low volume fractions as compared to the predicted values from Booth and R-R&C theoretical models. This unusual behaviour by silica dispersions were reported by Adamczyk *et al*. [5] and Laven & Stein [26] and both studies postulated a fuzzy gel-like structure for silica particles in aqueous environment as the explanation for such behaviour. Booth and R-R&C models showed similar qualitative behaviour to the experimental data at various pH and ionic strengths [16, 28, 66]. The R-R&C model showed up to 4% improved intrinsic viscosities and more than double PEE coefficient, p compared to Booth model. This may be due to the restrictions of small double layers and zeta potential (< 25.4) invalidating Booth model for most of the studied conditions. Instead, the R-R&C model is intended to be valid for non-dilute suspensions and arbitrary zeta potentials, even for the cases of overlapping of neighbour EDL's. Also further studying p for both models compared to the experimental data showed a consistent ratio of p_{exp} / $p_{R\text{-}R\&C}$ which was not the case for Booth model. This enabled the R-R&C model to predict the low volume fraction viscosities quite accurately for silica X30 particles by introducing a simple correction factor in $p_{R\text{-}R\&C}$.

For the high volume fraction studies, firstly, the electroviscous R-R&C model [22, 28] was investigated to explore its ability to predict the experimental results for different pH and ionic strength conditions. This model predicts the viscosity of a concentrated colloidal suspension of charged spherical particles including electroviscous effects linked to electric body forces in the double layers, and possible overlapping between adjacent double layers of neighbor particles. It was observed that the R-R&C model predicts values well below the experimental data. Also, the R-R&C hard sphere results (no electroviscous effects included) were displayed for the same cases which showed that the complete R-R&C prediction hardly differs from the simpler hard sphere one. These results showed similar behavior to the low volume fraction viscosities in which the R-R&C model predictions are well below the experimental values even for the pH5, 30mM ionic strength case.

To explain the discrepancies found between experiments and the R-R&C model, composite core/shell silica particle model was explored. As reported in the literature [5, 26], some discrepancies with colloidal silica particles between experiment and theory led to the postulation of a fuzzy, gel-like layer forming around the silica particles in aqueous conditions, responsible for the large specific viscosity deviations observed. This fact could explain the apparent particle density decrease for low ionic strength and high pH, and also that the thickness of the gel-like layer could apparently be correlated with the double-layer thickness.

To examine this core-shell approach, effective volume fractions were obtained two ways: by fitting the R-R&C hard sphere model to the experimental data, and also by the linear fits to the low volume fraction viscosity data, according to Adamczyk *et al's* [5]. It has been shown for all conditions that the R-R&C hard sphere model with effective volume fraction gives the best fits to the experimental specific viscosities, especially for 3 mM NaCl ionic strength. Likewise, Adamczyk *et al's* effective volume fraction does not seem to be a good approach for the high volume fraction studies for pHs larger than 5. Also the well-known K-D model was compared to the high volume fraction data, where the majority of the K-D fits overestimated the viscosity and were not good enough for adjusting our experiments.

In order to find possible correlations with such properties, the ratios of the thickness of the gel-like layer to the particle radius were displayed for all experimental conditions of zeta potential, pH and ionic strength according to the three approaches described. From the thickness ratio as a function of zeta potential at fixed ionic strength study, for both ionic strengths, 3 and 30 mM NaCl, the thickness ratio increases with zeta potential for all approaches. Remarkably, the K-D model generally showed the largest thickness ratios which implied an overestimation in comparison with the R-R&C approach. The Adamczyk *et al*'s approach on the other hand showed the smallest ratios which indicated and underestimation compared to the R-R&C model. For fixed ionic strengths, it is quite reasonable that the larger the surface potential the thicker the charged gel-like layer surrounding the bare particle.

Finally, the thickness ratio as a function of ionic strength was studied for fixed pH. Overall the thickness ratio decreased with ionic strength which was probably an effect of the well-

known double layer compression with the increase of ionic strength that partially compresses the charged gel-like layer.

In summary, for the present set of experiments with X30 Silica, it can be concluded that the present R-R&C hard sphere model suffices to match appreciably well the experimental viscosities if effective volume fractions are assumed. Such effective volume fractions are linked to the postulation of a fuzzy, gel-like structure for the colloidal silica particles. In addition, some correlations between the thickness ratio of the silica particles and pH, zeta potential or ionic strength have been found that might be correlated with the double layer thickness.

Acknowledgements

This work was performed in Swansea University and supported by the college of engineering.

References

[1] S.U.S. Choi, J.A. Eastman, Enhancing thermal conductivity of fluids with nanoparticles, ; Argonne National Lab., IL (United States)1995.
[2] H.E. Bergna, W.O. Roberts, Colloidal Silica: Fundamentals and Applications, 2006.
[3] R.K. Iler, The Chemistry of Silica: Solubility, Polymerization, Colloid and Surface Properties, and Biochemistry, 1979.
[4] J. Stone-Masui, A. Watillon, Electroviscous effect in dispersions of monodisperse polystyrene lattices, J. Colloid Interface Sci. 28 (1968) 187-202.
[5] Z. Adamczyk, B. Jachimska, M. Kolasinska, Determination of the structure of colloid silica determined by viscosity measurements, J. Colloid Interface Sci. 273 (2004) 668-674.
[6] F.J. Rubio-Hernández, M.F. Ayúcar-Rubio, J.F. Velázquez-Navarro, F.J. Galindo-Rosales, Intrinsic viscosity of SiO2, Al2O3 and TiO2 aqueous suspensions, Journal of Colloid and Interface Science 298 (2006) 967-972.
[7] F.J. Rubio-Hernandez, A.I. Gomez.-Merino, E. Ruiz-Reina, C. Carnero-Ruiz, The primary electroviscous effect of polystyrene lattices, Colloids Surf., A 140 (1998) 295-298.

[8] F.J. Rubio-Hernandez, A.I. Gomez.-Merino, E. Ruiz-Reina, M.J. Garcia-Salinas, An experimental test of booth's primary electroviscous effect theory, J. Colloid Interface Sci. 255 (2002) 208-213.
[9] W.R. Bowen, P.M. Williams, Prediction of the rate of cross-flow ultrafiltration of colloids with concentration-dependent diffusion coefficient and viscosity - theory and experiment, Chem. Eng. Sci. 56 (2001) 3083-3099.
[10] R.J. Hunter, Zeta Potential in Colloid Science. Principles and Applications, 3 ed., Academic Press, London, 1981.
[11] R.J. Hunter, Introduction to Modern Colloid Science, Oxford University Press, New York, 1993.
[12] R.J. Hunter, Foundations of Colloid Science, Oxford University Press2001.
[13] W.B. Russel, D.A. Saville, W.R. Schowalter, Colloidal Dispersions, Cambridge University Press, Cambridge, 1989.
[14] B.E. Conway, A. Dobry-Duclaux, Rheology: Theory and applications, Academic Press, New York and London, 1960.
[15] M.v. Smoluchowski, Theoretische bemerkungen uber die viskositat der Kolloide, Kolloid Z. 18 (1916) 190.
[16] F. Booth, The electroviscos effect for suspensions of solid spherical particles, Proc. Roy. Soc. London A 203(1075) (1950a) pp. 533-551.
[17] I.G. Watterson, L.R. White, Primary electroviscous effect in suspensions of charged spherical particles, J. Chem. Soc., Faraday Trans. II 77 (1981) 1115.
[18] J.D. Sherwood, The primary electroviscous effect, Cambridge University, 1978.
[19] J.D. Sherwood, Primary electroviscous effect in a suspension of spheres, J. Fluid Mech. 101 (1980) 609.
[20] W.B. Russel, Review of the role of colloidal forces in the rheology of suspensions, J. Rheology 24 (1980) 287-317.
[21] M.G. Bell, G.C. Peterson, Calculation of the electric double-layer force between unlike spheres., J. Colloid Interface Sci. 41 (1972) 542.
[22] E. Ruiz-Reina, P. Garcia-Sanchez, F. Carrique, Electroviscous effect for moderately concentrated colloidal suspensions under overlapping conditions, J. Phys. Chem. B 109 (2005) 5289 - 5299.
[23] H. Ohshima, Primary electroviscous effect in a dilute suspension of charged mercury drops, Langmuir 22 (2006a) 2863 - 2869.
[24] H. Ohshima, Primary electroviscous effect in a moderately concentrated suspension of charged spherical colloidal particles, Langmuir 23 (2007) 12061 - 12066.
[25] W. Krasny-Ergen, Untersuchungen über die viskosität von suspensionen und lösungen. 2. Zur theorie der elektroviskosität, Kolloid Z. 74 (1936) 172.
[26] J. Laven, H.N. Stein, The electroviscous behaviour of aqueous dispersions of amorphous silica (Ludox), J. Colloid Interface Sci. 238 (2001) 8-15.
[27] H.B. Bull, The electroviscous effect in egg albumin solutions, Trans. Faraday Soc. 36(1) (1940) 80-84.

[28] E. Ruiz-Reina, F. Carrique, Electroviscous effect of concentrated suspensions in salt-free media: water dissociation and CO_2 influence, J. Colloid Interface Sci. 345 (2010) 538-546.
[29] D. Quemada, Concentrated Colloidal Suspensions at Low Ionic Strength: A Hard-Sphere Model of Zero Shear Viscosity, Involving the Hard-Sphere Phase Transitions, EPL (Europhysics Letters) 25(2) (1994) 149.
[30] C. Allain, M. Cloitre, B. Lacoste, I. Marsone, Viscosity renormalization in colloidal suspensions, The Journal of Chemical Physics 100(6) (1994) 4537-4542.
[31] M. Swaroop, J.F. Brady, The bulk viscosity of suspensions, Journal of Rheology 51(3) (2007) 409-428.
[32] J.S. Chong, E.B. Christiansen, A.D. Baer, Rheology of concentrated suspensions., J. Appl. Polym. Sci. 15 (1971) 2007.
[33] R. Mondragon, J. Enrique Julia, A. Barba, J.C. Jarque, Determination of the packing fraction of silica nanoparticles from the rheological and viscoelastic measurements of nanofluids, Chemical Engineering Science 80 (2012) 119-127.
[34] M. Pishvaei, C. Graillat, P. Cassagnau, T.F. McKenna, Modelling the zero shear viscosity of bimodal high solid content latex: Calculation of the maximum packing fraction, Chem. Eng. Sci. 61 (2006) 5768-5780.
[35] I.M. Krieger, T.J. Dougherty, A mechanism for non-Newtonian flow in suspensions of rigid spheres, Trans. Soc. Rheol. 3 (1959) 137-152.
[36] I.M. Krieger, M. Eguiluz, The second electroviscous effect in polymer lattices Trans. Soc. Rheol. 20 (1976) 29.
[37] Y.S. Papir, I.M. Krieger, Rheological studies on dispersions of uniform colloidal spheres: II. Dispersions in nonaqueous media, J. Colloid Interface Sci. 34 (1970) 126.
[38] F. Candau, P. Buchert, I. Krieger, Rheological studies on Inverse Microlatices, Journal of Colloid and Interface Science 140(2) (1990) 466.
[39] M.E. Woods, I.M. Krieger, Rheological studies on dispersions of uniform colloidal spheres I. Aqueous dispersions in steady shear flow, J. Colloid Interface Sci. 34 (1970) 91.
[40] J.C. van der Werff, C.G. de Kruif, Hard sphere colloidal dispersions: the scaling of rheological properties with particle size, volume fraction, and shear rate, J. Rheorlogy 33 (1989) 421-454.
[41] R.J. Simha, A treatment of the viscosity of concentrated suspensions, J. Appl. Phys. 23 (1952) 1020-1024.
[42] S.R. Deshiikan, K.D. Papadopoulos, Modified Booth equation for the calculation of zeta potential, Colloid Polym. Sci. 276 (1998) 117-124.
[43] E. Huckel, The cataphoresis of the sphere, Physik. Z. 25 (1924) 204.
[44] R.W. O'Brien, R.J. Hunter, The electrophoretic mobility of large colloidal particles, Canad. J. Chem. 59 (1981) 1878.
[45] R.W. O'Brien, L.R. White, Electrophoretic mobility of a spherical colloidal particle, J. Chem. Soc., Faraday Trans. II 74 (1978) 1607.

[46] M.v. Smoluchowski, Handbuch der Elektrizität und des Magnetismus (Graetz, L), Leipzig, J.A. Barth1921.
[47] H. Ohshima, A simple expression for the electrophoretic mobility of charged mercury drops, J. Colloid Interface Sci. 189 (1997) 376 - 378.
[48] F. Booth, The cataphoresis of spherical, solid non-conducting particles in a symmetrical electrolyte, Proc. Roy. Soc. London A 203 (1950b) 514.
[49] A. Einstein, Eine neue bestimmung der moleküldimensionen, Ann. Phys. 19 (1906) 289.
[50] F. Booth, Theory of electrokinetic effects, Nature 161 (1948) 83-86.
[51] W. Krasney-Ergen, Kolloidzeit. 74 (1936) 172.
[52] B.N. Finkelstein, M.P. Chursin, Acta Physicochim URSS 17 (1942) 1.
[53] N. Street, A simple derivation of an electroviscous equation, J. Colloid Sci. 13 (1958) 288.
[54] J.R. Whitehead, A note on street's electroviscous equation, J. Colloid Interface Sci. 30 (1969) 424.
[55] J.D. Sherwood, E.J. Hinch, The primary electroviscous effect in a suspension of spheres with thin double layers, J. Fluid Mech. 132 (1983) 337-347.
[56] J.D. Sherwood, F.J. Rubio-Hernandez, E. Ruiz-Reina, The Primary Electroviscous Effect: Thin Double Layers and a Stern Layer, J. Colloid Interface Sci. 228 (2000) 7-13.
[57] W.A. Ducker, T.J. Senden, R.M. Pashley, Measurement of forces in liquids using a force microscope., Langmuir 8 (1992) 1831-1836.
[58] A.S. Dukhin, T.G.M. van de Ven, A spherical particle surrounded by a thin double layer in a simple shear flow, J. Colloid Interface Sci. 158 (1993) 85-95.
[59] A.S. Dukhin, T.G.M. van de Ven, Trajectories of charged tracer particles around a charged sphere in a simple shear flow, J. Fluid Mech. 263 (1994) 185-205.
[60] S.S. Dukhin, B.V. Derjaguin, Surface and Colloid Science, John Wiley, New York, 1974.
[61] T.G.M. van de Ven, Colloidal Hydrodynamics, Academic Press, London, 1989.
[62] T.G.M. van de Ven, Electroviscous phenomena in colloidal dispersions, Chem. Eng. Sci. 56 (2001) 2947-2955.
[63] J.J. Happel, Viscosity of Suspensions of Uniform Spheres, J. Appl. Phys. 28 (1957) 1288-1292.
[64] J.D. Sherwood, Cell model for the primary electroviscous effect, J. Chem. Phys. 111 (2007) 3370-3378.
[65] E. Ruiz-Reina, F. Carrique, F.J. Rubio-Hernandez, A.I. Gomez.-Merino, P. Garcia-Sanches, Electroviscous effect of moderately concentrated colloidal suspensions, J. Phys. Chem. B 107 (2003) 9528.

[66] E. Ruiz-Reina, F. Carrique, Electroviscous Effect of Concentrated Colloidal Suspensions in Salt-Free Solutions, The Journal of Physical Chemistry C 111(1) (2007) 141-148.
[67] R. Ball, P. Richmond, Dynamics of colloidal dispersions, J. Phys. Chem. Liquids 9 (1980) 99-116.
[68] K. Monkos, Determination of some hydrodynamic parameters of ovine albumin solutions using viscometric measurements, J. Biol. Phys. 31 (2005) 219-232.
[69] A.A. Kozinski, E.N. Lightfoot, Protein ultrafiltration: A general example of boundary layer filtration, AIChE J. 18 (1972) 1030–1040.
[70] K. Monkos, Viscosity of BSA aqueous solutions as a function of temperature and concentration, Int. J. Biol. Macromol. 18 (1996) 61-68.
[71] BS 188, Methods for determination of the viscosity of liquids., (1977).
[72] A. Einstein, Berichtigung zu meiner arbeit: Eine neue bestimmung der moleküldimensionen, Ann. Phys. 34 (1911) 591.
[73] G.K. Batchelor, J. Fluid Mech. 83 (1997) 97.

7: Electronic Supplementary Material

Click here to download 7: Electronic Supplementary Material: Revised Supporting Information - decoded.docx